



Uropathogenic *Escherichia coli* Shows Antibiotic Tolerance and Growth Heterogeneity in an *In Vitro* Model of Intracellular Infection

Ivana Kerkez,^{a,b} Paul M. Tulkens,^a Tanel Tenson,^b  Françoise Van Bambeke,^a  Marta Putrinš^b

^aPharmacologie cellulaire et moléculaire, Louvain Drug Research Institute, Université catholique de Louvain, Brussels, Belgium

^bInstitute of Technology, University of Tartu, Tartu, Estonia

Françoise Van Bambeke and Marta Putrinš contributed equally as senior authors of the paper.

ABSTRACT Uropathogenic *Escherichia coli* (UPEC), the major causative agent of urinary tract infections, can invade different types of host cells. To compare the pharmacodynamic properties of antibiotics against intra- and extracellular UPEC, an *in vitro* model of intracellular infection was established in J774 mouse macrophages infected by the UPEC strain CFT073. We tested antibiotics commonly prescribed against urinary tract infections (gentamicin, ampicillin, nitrofurantoin, trimethoprim, sulfamethoxazole, and ciprofloxacin) and the investigational fluoroquinolone finafloxacin. The metabolic activity of individual bacteria was assessed by expressing the fluorescent reporter protein TIMERbac within CFT073. Concentration-response experiments revealed that all tested antibiotics were much less effective against intracellular bacteria than extracellular ones. Most antibiotics, except fluoroquinolones, were unable to reach a bactericidal effect intracellularly at clinically achievable concentrations. Ciprofloxacin and finafloxacin killed 99.9% of extracellular bacteria at concentrations around the MIC, while for intracellular bacteria, concentrations more than 100× over the MIC were required to achieve a bactericidal effect. Time-kill curves showed that finafloxacin was more rapidly bactericidal in acidic medium than at neutral pH, while the reverse observation was made for ciprofloxacin. Intracellularly, kill curves showed biphasic kinetics for both fluoroquinolones, suggesting the presence of drug-tolerant subpopulations. Flow cytometry analysis of TIMERbac fluorescence revealed a marked heterogeneity in intracellular growth of individual bacteria, suggesting that the presence of subpopulations reaching a state of metabolic dormancy was the main reason for increased antibiotic tolerance of intracellular UPEC.

KEYWORDS TIMERbac, UPEC, UTI, flow cytometry, fluorescent reporter, fluoroquinolones, intracellular infection, macrophages, persisters, pharmacodynamics

The *Escherichia coli* species contains both commensal bacteria living in human gut as well as pathogenic strains causing infections like gastroenteritis, Crohn's disease, hemorrhagic colitis, neonatal meningitis, and urinary tract infections (UTIs). Uropathogenic *Escherichia coli* (UPEC) is the most prevalent causative agent of UTIs (1). While often characterized as an extracellular pathogen, many studies have revealed the ability of this bacterium to invade host bladder and renal epithelial cells as well as macrophages as a part of urinary tract pathogenesis (2–4). Once bacteria have been internalized, the intracellular environment provides them protection against host defensive mechanisms and, in some cases, antibiotic activities, which together are proposed to contribute to the colonization and persistence of UPEC in the urinary tract (1, 5, 6). The resurgence of persistent intracellular bacterial reservoirs may in turn explain the recurrence of UTIs (7, 8). It is important to emphasize that besides the persistence of bacteria in bladder epithelium, recurrent UTIs

Citation Kerkez I, Tulkens PM, Tenson T, Van Bambeke F, Putrinš M. 2021. Uropathogenic *Escherichia coli* shows antibiotic tolerance and growth heterogeneity in an *in vitro* model of intracellular infection. *Antimicrob Agents Chemother* 65:e01468-21. <https://doi.org/10.1128/AAC.01468-21>.

Copyright © 2021 American Society for Microbiology. All Rights Reserved.

Address correspondence to Françoise Van Bambeke, francoise.vanbambeke@uclouvain.be, or Marta Putrinš, marta.putrins@ut.ee.

Received 25 July 2021

Returned for modification 11 August 2021

Accepted 22 September 2021

Accepted manuscript posted online

27 September 2021

Published 17 November 2021

can also be caused either by infection by a new strain or reinfection by the same strain persisting in the gastrointestinal tract (9, 10).

Enhanced survival of intracellular bacteria has been studied for several bacterial species that cause persistent infections. In many cases intracellular persistence is attributed to the acquisition of a so-called persister phenotype (11–13). Persisters are subpopulations of bacteria that remain susceptible but do not respond to antibiotic treatment due to metabolic adaptation. They do not multiply and revert to a normal phenotype when the antibiotic pressure has been removed (14). *In vitro* experiments have shown that persisters can also serve as a source of *de novo* resistance mutations (15, 16).

When dealing with the treatment of intracellular bacterial infections, many obstacles for antibiotics to act on their target need to be taken into consideration. These include the capacity of the drug to reach the bacteria in the infected subcellular compartment or to express its activity at the local pH of this infected compartment as well as to effectively target metabolically inactive bacteria (17, 18). Pharmacodynamic indices are indeed different for many species when intracellular bacteria are compared to extracellular bacteria growing in pure culture (19–23). Previous work with UPEC showed that bacteria can persist intracellularly in the presence of antibiotics with different mechanisms of action, and that some antibiotics, such as nitrofurantoin and fluoroquinolones, were more efficient than others at intracellular bacterial eradication (24, 25). However, the earlier studies lack a direct comparison with extracellular bacteria and measurement of pharmacodynamic indices.

The commonly prescribed first line of UTI treatment antibiotics includes nitrofurantoin, trimethoprim-sulfamethoxazole, and fosfomycin, while the second line of treatment makes use of fluoroquinolones, beta-lactams, or, sometimes, aminoglycosides (26). In the present study, we investigated the pharmacodynamic properties of commonly prescribed antibiotics and of a novel fluoroquinolone, finafloxacin, currently in clinical development for the treatment of complicated urinary tract infections (27). Finafloxacin shows the unusual property for a fluoroquinolone of being more active at acidic pH against different bacterial species because it accumulates to higher levels inside bacteria under these conditions (21, 28). This has been ascribed to the fact that finafloxacin is predominantly present as a diffusible zwitterion at acidic pH (28). We compared the activity of different antibiotics against extra- and intracellular UPEC in growth medium and a macrophage cell culture assay, respectively. We used a comprehensive approach that includes concentration- or time-kill curves. Concentration-kill curves allowed us to determine pharmacodynamic indices such as relative potencies and maximal efficacies that characterize the activity profile of antibiotics (29). Time-kill curves were used to reveal the existence of antibiotic-tolerant subpopulations. In parallel, bacteria expressing a fluorescent reporter protein (TIMERbac) were used to analyze growth dynamics and the metabolic activity of intracellular bacteria at the single bacterial cell level. We found that the efficacy of all antibiotics was markedly impaired intracellularly, leaving an untouched pool of dormant or metabolically inactive bacteria that survived antibiotic treatment even at high concentrations.

RESULTS

Antibiotic susceptibility testing. Antibiotic MICs for the CFT073 strain were determined in Mueller-Hinton broth (MHB) and Dulbecco's modified Eagle's medium (DMEM), adjusted to neutral pH 7.4 or acidic pH 5.5 to mimic the pH of intracellular vacuoles (Table 1). In DMEM at neutral pH, MICs were the same or 1 doubling dilution higher than those measured in MHB, except for nitrofurantoin (2 dilutions higher). Lowering the pH of DMEM increased marginally (0 to 1 doubling dilution) the MIC of ampicillin and trimethoprim, 1 to 2 doubling dilutions for gentamicin and sulfamethoxazole, and 4 doubling dilutions for ciprofloxacin. In contrast, the MIC of finafloxacin was 4 doubling dilutions lower at acidic pH than at neutral pH. For most antibiotics, the highest concentration tested in further experiments corresponded to 100× the MIC measured in DMEM at pH 7.4. For fluoroquinolones, the highest tested

TABLE 1 MICs of antibiotics in MHB and DMEM supplemented by 10% FBS at pH 5.5 and 7.4

Antibiotic	MIC ^a (mg/liter)		DMEM, pH 7.4		DMEM, pH 5.5		Highest concn tested (mg/liter)	C _{max} (mg/liter) in serum		C _{max} (mg/liter) in urine		Reference
	MHB, pH 7.4	DMEM, pH 7.4	DMEM, pH 7.4	DMEM, pH 5.5	C _{max} (dosing)	Reference		C _{max} (dosing)	Reference			
Ampicillin (AMP)	2	4	4	8 (4-8)	400	3.2 (250 mg single dose)	52	185.5 (500 mg single dose)	53			
Gentamicin (GEN)	2	1	0.5 (0.5-1)	4	100	5.4 (3-4 mg/kg/day)	54	72 (0.7-1.2 mg/kg/day)	55			
Trimethoprim (TMP)	0.25	4 (2-4)	16 (16-32)	1 (0.5-1)	50	6 (300 mg/day)	56	41.5 (200 mg single dose)	57			
Sulfamethoxazole (SMX)	8	4 (4-8)	0.016	8 (4-8)	400	46.3 (800 mg every 8 h)	58	80.2 (800 mg single dose)	59			
Nitrofurantoin (NIT)	4 (4-8)	0.5 (0.25-0.5)	0.0312	4 (4-8)	160	1.81 (100 mg every 6h; loading dose 200 mg)	60	230 (100 mg every 6 h)	61			
Ciprofloxacin (CIP)	0.016	0.5 (0.25-0.5)	0.016	0.25 (0.125-0.25)	150	2.30 (500 mg single dose)	62	268 (500 mg single dose)	62			
Fluoroquinolone (FIN)	0.25 (0.125-0.25)	0.5 (0.25-0.5)	0.0312	0.0312	150	14 (800 mg single dose)	63	180 (800 mg/day)	64			

^aMIC was determined at least 3 times for each condition. In case of inconsistencies, the most frequent MIC value (together with detected range in parentheses) is shown.

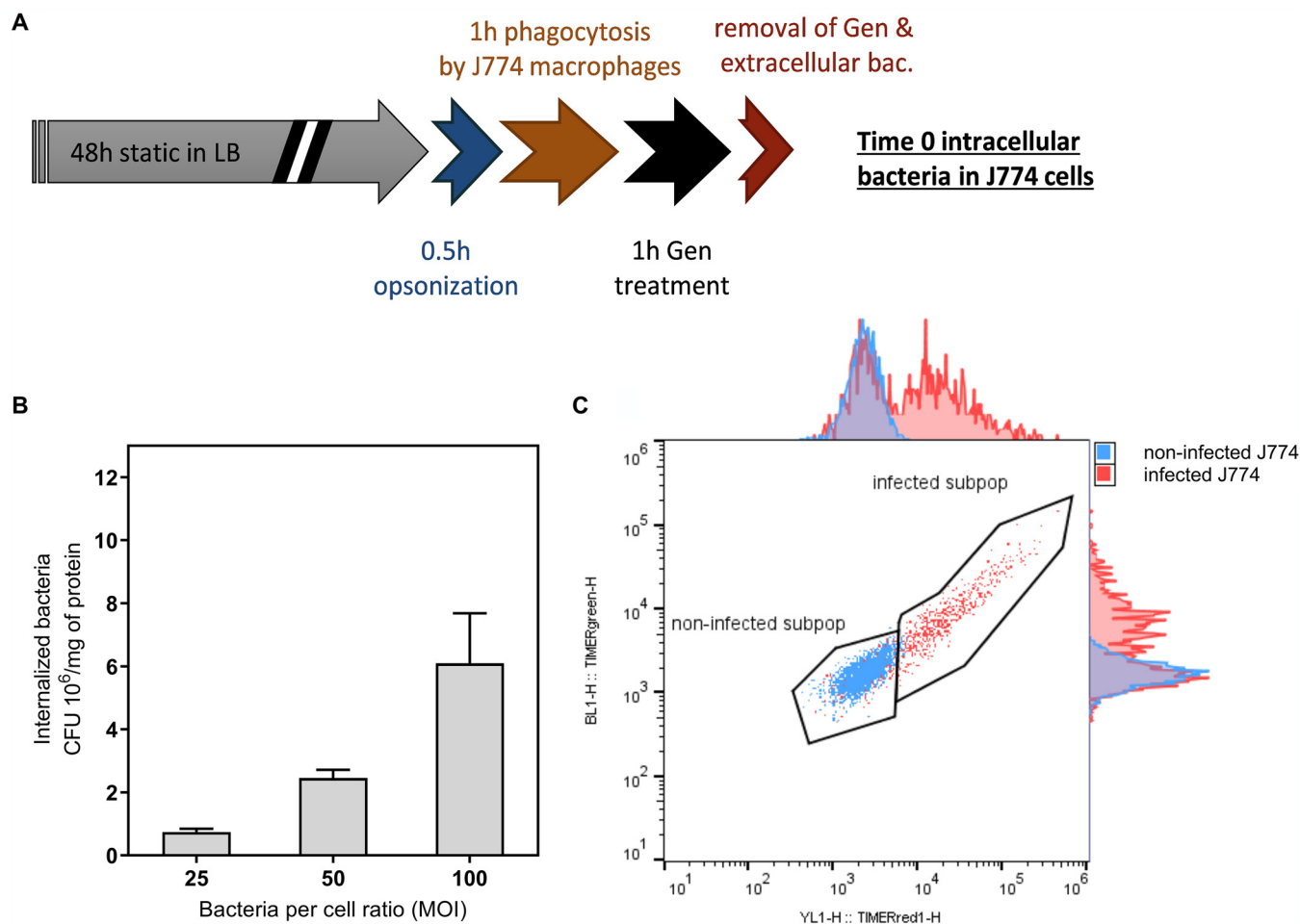


FIG 1 J774 macrophage infection model for pharmacodynamic evaluation of antibiotics against intracellular *E. coli* CFT073. (A) Schematic representation of infection protocol. Gentamicin (Gen) treatment (100 mg/liter) was used to remove of the extracellular bacteria. (B) Number of intracellular bacteria at time zero for different infection loads indicated as multiplicity of infection (MOI). Results are mean values \pm standard deviations from at least 3 experiments (each experiment was done in triplicate). (C) Representative flow cytometry analysis for one experiment of red and green fluorescence in J774 macrophages after infection by CFT073 expressing TIMERbac and elimination of extracellular gentamicin (time zero in panel A). Overlay of control cells (noninfected; blue color) and macrophages that were exposed to bacteria (time zero in panel A; red color) gives two distinct subpopulations; one with high red fluorescence (infected cells) and another that overlaps with the control (noninfected cells).

concentration was 150 mg/liter, which was much higher than the human C_{\max} in serum but similar to the measured or predicted human C_{\max} in urine (Table 1).

Setting up an *in vitro* intracellular model of infection to study intracellular antibiotic activity. To establish a model for pharmacodynamic studies of antibiotic activity, the infection of mouse macrophage-like cell line J774 was carried out using the UPEC strain CFT073 at different bacterium/cell ratios (MOI, or multiplicity of infection). This cell line was selected because it is quite permissive toward a variety of intracellular infectious agents, allowing detailed analysis of the effects of antibiotics without too much interference from the host-derived mechanisms of defense (30). Bacteria were carrying a plasmid expressing reporter-protein TIMERbac to enable visualization and subsequent analyses of the physiological state of each bacterium.

Using a previously described experimental setup (Fig. 1A) (30), we tested bacterial internalization at different MOIs (bacterium/cell ratio). As shown in Fig. 1B, the number of internalized bacteria increased in proportion to the extracellular inoculum. An MOI of 50 was selected for further experiments, because we aimed to reach an initial infection level of approximately 10^6 CFU per milligram of protein, which allows us to later monitor the killing of intracellular bacteria by antibiotics. Macrophage cell viability at an MOI of 50 was also determined, with $91.6\% \pm 5.9\%$ of cells remaining viable based on a Trypan blue exclusion test.

Next, to determine the proportion of infected cells in our experimental setup, we measured the signal of the fluorescent reporter protein TIMERbac, expressed by internalized bacteria, by analyzing formaldehyde-fixed macrophages with flow cytometry. The TIMERbac protein is a tetramer bearing green and red fluorophores. Due to its branched maturation pathway, green fluorophores appear earlier than slowly maturing red fluorophores. Therefore, in dividing cells, the slow-maturing red form is diluted out, and cells have a higher green/red fluorescence ratio. Conversely, both red and green fluorescence accumulate in nondividing cells (see Fig. S1 in the supplemental material) (31). This is what we observed for overnight cultures of bacterial cells. J744 macrophage cells have relatively high autofluorescence, especially in the green light range. Therefore, infected macrophages were distinguished mostly by higher red fluorescence coming from the bacterial reporter protein TIMERbac than for noninfected control cells (Fig. 1C). This feature was used to calculate the percentage of initially infected macrophages, which was $41.2\% \pm 16.6\%$ based on 3 different experiments with two replicates.

Intracellular localization and restricted growth of internalized bacteria. To visualize the localization of intracellular bacteria, infected macrophages were examined under a confocal microscope. Bacteria were identified via the signal emitted by the reporter protein TIMERbac in both the green and red channels. LysoSensor was used to localize the acidic vacuoles in the blue channel. Confocal microscopy pictures of infected macrophages at time zero revealed that bacteria were localized in round compartments with an acidic pH (Fig. 2A to C).

Next, we aimed to record quantitative data of the fluorescence levels of the TIMERbac reporter to determine whether intracellular bacteria are metabolically active and dividing within macrophages. To this aim, we analyzed intracellular bacteria versus extracellular bacteria in DMEM using flow cytometry. Extracellular bacteria (as a growth resumption control) were obtained from infected macrophages at the zero time point by lysing macrophages and inoculating the released bacteria into DMEM. Intracellular bacteria were obtained from macrophages grown in the presence of gentamicin at 3 mg/liter in the medium to prevent growth of any extracellular bacteria. Having the same population at the starting point allows us to compare multiplication rate of bacteria in the intra- and extracellular environments after 3 h of incubation using flow cytometry. Based on the measured fluorescence levels, bacteria were divided into three subpopulations (quartiles), Q1, Q2, and Q3 (Fig. 2D). Q1 corresponds to dividing bacteria for which the fluorescence of the red fluorophore has decreased over time, while the signal from the rapidly maturing green fluorophore has not decreased. Q2 denotes bacteria with relatively high green and red fluorescence that do not divide but maintain metabolic activity. Q3 represents bacteria for which red fluorescence dominates, which indicates that active protein synthesis has stopped (may correspond either to metabolically inactive or to already dead cells).

A comparative analysis shown in Fig. 2D and E revealed that at the 3-h time point, extracellular bacteria are dividing and metabolically active (prevalence of Q1 and Q2 subpopulations). In contrast, the proportion of Q3 cells increased intracellularly during the 3 h of incubation, suggesting strong growth inhibition in this environment (Fig. 2E).

Pharmacological comparison of antibiotics against extra- and intracellular bacteria. To compare antibiotic pharmacodynamics against extra- and intracellular bacteria, CFU numbers were determined after 24 h of exposure to drugs over a wide range of concentrations. For activity against extracellular bacteria in broth, only simple CFU determination was performed. For intracellular bacteria, infected macrophages were first washed to remove potential extracellular bacteria, and the CFU numbers determined from lysed host cells were normalized to the sample protein content. We suspected that if the antibiotic concentration in the growth medium is below the MIC, then killing of macrophages and release of extracellular bacteria to the surrounding medium can take place within 24 h. Therefore, after 24 h of incubation with different concentrations of gentamicin, we determined (i) the number of CFU growing from

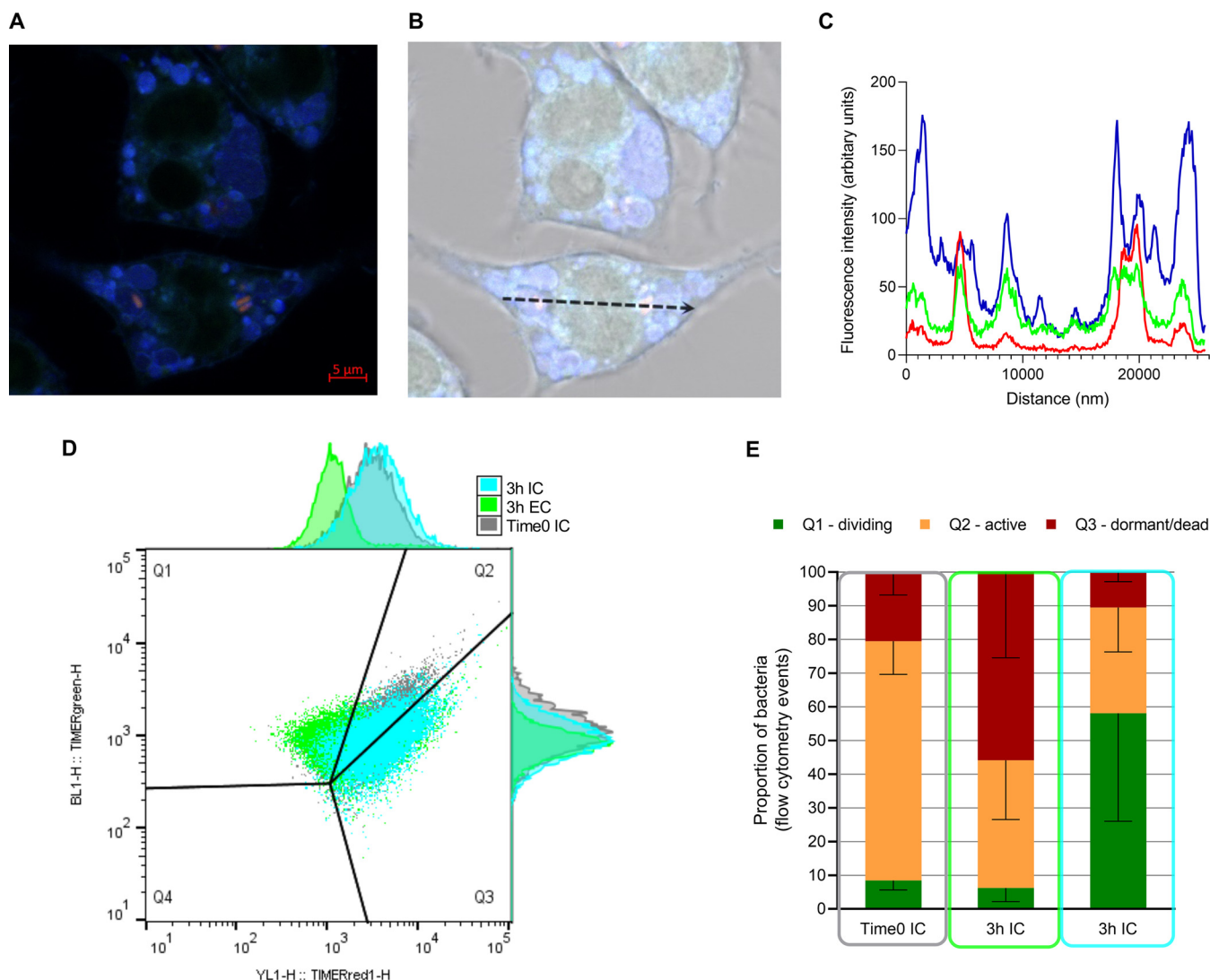


FIG 2 Fluorescent microscopy and flow cytometry analyses on bacterial growth and activity with TIMERbac reporter-protein. (A) Confocal microscopy image of infected macrophages at time zero with overlay of three pseudocolored channels. Blue color (Ex, 458 nm; Em, 474 to 554 nm) indicates signal from Lyso Sensor dye DND-189; green (Ex, 488 nm; Em, 493 to 533nm) and red color (Ex, 561 nm; Em, 566 to 616 nm) indicate signal from reporter protein TIMERbac. Intracellular bacteria are indicated with white arrows. (B) Fluorescent image is overlaid with transmitted light image from 488-nm laser, and the dotted line indicates the section from which quantitative fluorescence intensities are measured and presented in panel C. (C) Bacteria expressing TIMERbac protein (green and red fluorescence) are localized within acidic intracellular compartments (blue fluorescence). (D) Three bacterial subpopulations Q1, Q2, and Q3 detected by FACS by analyzing intracellular (IC) and extracellular (EC) control bacteria. Abundances of respective bacterial subpopulations (shown in percentages) are presented in panel E. Results are averages \pm standard deviations from three experiments with at least two parallels.

extracellular media; (ii) the number of macrophages; and (iii) macrophage viability based on a lactate dehydrogenase (LDH) assay.

As shown in Fig. 3A, the number of extracellular bacteria was very high under conditions where gentamicin concentrations were 0.003 mg/liter (below the MIC). This was accompanied by the change of color of the medium from red to yellow, indicating acidification resulting from bacterial growth. Importantly, at a gentamicin concentration of 1 mg/liter (i.e., the MIC in DMEM), we observed a high variability in the number of bacteria in medium between different experiments (Fig. 3A). Of note, the appearance of small colony variants of CFT073 were detected from samples incubated with gentamicin at 1 mg/liter but not with higher or lower concentrations (Fig. S2). Compared to the condition before infection, there was a significant decrease in macrophage cell number ($P = 0.02$) and viability (increase in LDH release; $P = 0.001$) when the gentamicin concentration was 0.003 mg/liter (Fig. 3A). Conversely, when the

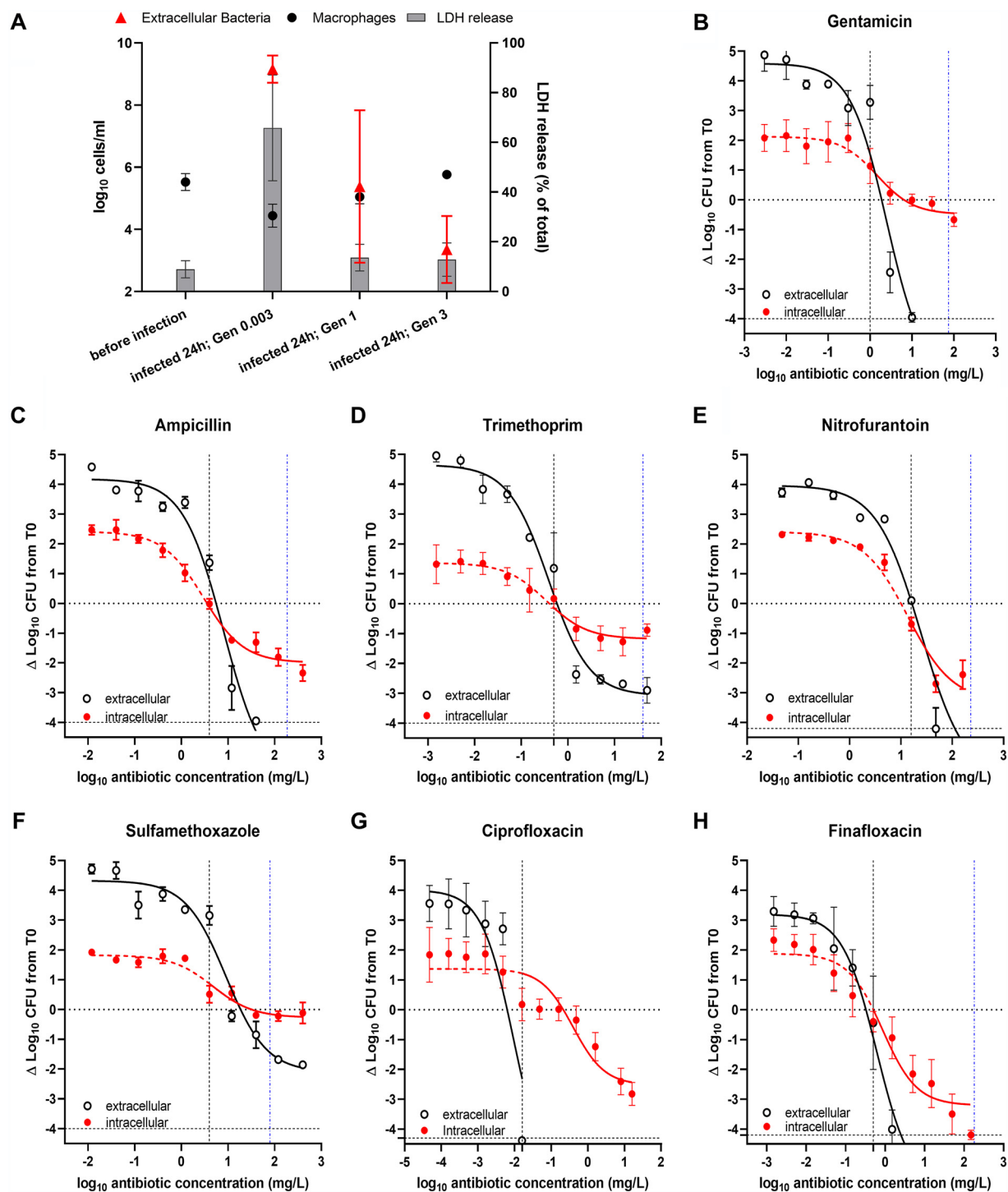


FIG 3 Antibiotic concentration-response curves for planktonic (extracellular) versus internalized (intracellular) bacteria after 24 h of incubation. (A) The effect of three different gentamicin concentrations on extracellular contamination (bacterial CFU/ml, red triangles); total number of macrophages per ml of DMEM after trypsinization (black dots) and LDH release (gray bars). All three parameters were acquired from the same well. (B to H) Activity of antibiotics against extracellular (open symbols, black line) and intracellular bacteria (closed symbols, red solid line); apparent intracellular bacteria counts at sub-MIC concentrations are presented with a dotted red line) were expressed in changes \log_{10} CFU units from time zero to 24 h, and the concentrations tested (mg/liter) are presented in \log_{10} scale. The first vertical black-dotted line corresponds to the MIC of the antibiotic as measured in DMEM at pH 7.4, and the second vertical blue-dotted line corresponds to the C_{max} of the drug in patient urine. Results are mean values \pm standard errors of the means (SEM) from at least three experiments (each experiment was done in triplicate). The horizontal dotted lines correspond to the initial inoculum and to the limit of detection, respectively.

TABLE 2 Pharmacodynamic parameters of concentration-response curve

Antibiotic	Extracellular				Intracellular			
	E_{\max}^a	KC_{90}^b	KC_{99}^b	R^2^c	E_{\max}^a	KC_{90}^b	KC_{99}^b	R^2^c
Ampicillin	<−4	8.3	12.3	0.95	−1.995 (−2.316 to −1.688)	19.1	NA ^d	0.94
Trimethoprim	−3.08 (−3.559 to −2.614)	1.1	2.4	0.96	−1.181 (−1.509 to −0.873)	4.5	NA	0.87
Sulfamethoxazole	−2.103 (−2.703 to −1.542)	43.7	555.9	0.95	−0.272 (−0.589 to 0.015)	NA	NA	0.86
Gentamicin	<−4	2.8	4.0	0.92	−0.491 (−0.728 to −0.268)	NA	NA	0.82
Nitrofurantoin	<−4	24.6	37.0	0.94	−3.288 (−3.974 to −2.678)	20.4	46.8	0.93
Ciprofloxacin	<−4	0.01	0.01	0.78	−2.527 (−3.271 to −1.842)	0.6	2.5	0.78
Fluoroquinolone	<−4	0.5	0.8	0.93	−3.208 (−3.663 to −2.795)	1.1	2.7	0.89

^aMaximal reduction in bacterial counts (\log_{10} difference compared to initial CFU) extrapolated from the Hill equation of concentration-response curves shown in Fig. 3; 95% confidence interval is given in parentheses.

^bConcentrations in mg/liter resulting in 90 and 99% reduction from initial inoculum calculated from the Hill equation of concentration-response curves shown in Fig. 3.

^cGoodness-of-fit curves shown in Fig. 3.

^dNA, not applicable.

extracellular growth of bacteria was prevented by gentamicin at a concentration 3× higher than its MIC (3 mg/liter), the extracellular contamination was much lower, and the viability of macrophages was not affected and was comparable to that of the non-infected control (Fig. 3A). Therefore, we can conclude that in our infection model, killing of macrophages by intracellular bacteria is only negligible when the antibiotic concentration is higher than its MIC, thereby preventing the growth of extracellular bacteria that have escaped from the macrophages. With lower antibiotic concentrations, the contamination of the samples by extracellular bacteria cannot be excluded despite the extensive washing of macrophages before studying the intracellular bacteria, which is the reason why the fit for the intracellular concentration-response curves was represented by a dotted line for these sub-MIC antibiotic concentrations (Fig. 3).

Full pharmacological dose-response curves were obtained for seven drugs that are or can be used for the treatment of UTIs: gentamicin, ampicillin, trimethoprim, nitrofurantoin, sulfamethoxazole, ciprofloxacin, and fluoroquinolone (Fig. 3). The concentrations we tested covered a broad range, corresponding to 0.003× up to 100× their MIC values (determined in DMEM, pH 7.4) and including levels that can be reached in the urine of treated patients (Table 1).

CFU data were used to fit Hill equation curves to derive a key pharmacodynamic parameter describing relative efficacy, namely, E_{\max} (maximal reduction of inoculum extrapolated for an infinitely large concentration). In addition, we calculated the drug killing concentration, KC_{90} and KC_{99} , resulting in 90 and 99% reduction from the initial inoculum, respectively. Both predicted E_{\max} and interpolated KC_{90} and KC_{99} are presented in Table 2. In this analysis, the Hill factor was fixed to −1, because there was no *a priori* reason to consider cooperative effects in antibiotic action.

Clearly, all antibiotics were more effective against extracellular bacteria than against intracellular bacteria (more negative E_{\max}) (Fig. 3B to H). Extracellularly, a bactericidal effect (99.9% of killing) was achieved at the highest tested concentration for all drugs except sulfamethoxazole, which reduced the initial inoculum of 99%. Fluoroquinolones, especially ciprofloxacin, were the most potent, allowing samples to reach the limit of detection at their MIC or low multiples thereof. Intracellularly, the most effective drugs were nitrofurantoin and fluoroquinolone, with an E_{\max} surpassing 99.9% killing, followed by ciprofloxacin, with an E_{\max} over 99% killing. Ampicillin and trimethoprim were also able to reduce intracellular bacterial levels but did not reach the bactericidal threshold over the time and concentrations we tested. Gentamicin and sulfamethoxazole only caused marginal reductions in intracellular counts at the highest concentration tested. KC_{90} were, in general, similar or slightly higher (2- to 3-fold) extra- and intracellularly, except for ciprofloxacin, which was less potent intracellularly, and gentamicin and sulfamethoxazole, which did not reach a 90% reduction against intracellular bacteria over the range of concentrations investigated. KC_{99} was also similar or slightly higher intracellularly for nitrofurantoin and fluoroquinolone and 250-fold higher for ciprofloxacin.

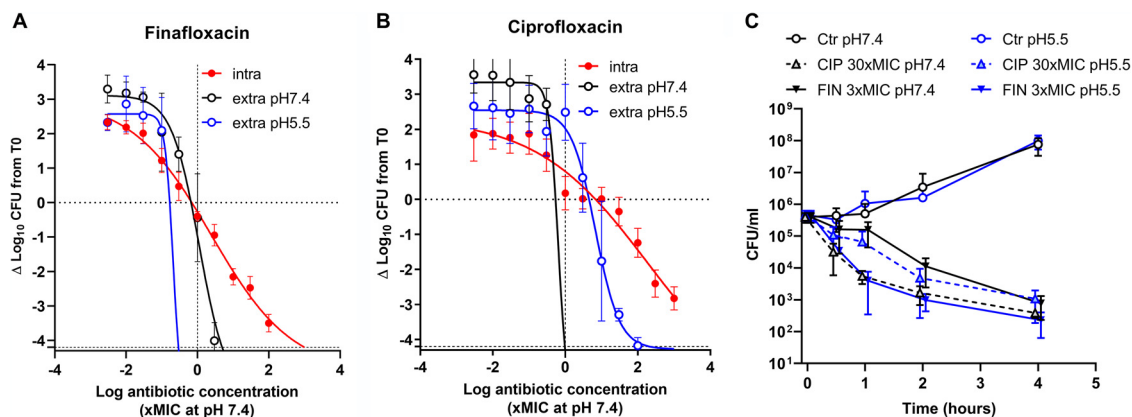


FIG 4 Effect of pH on ciprofloxacin and finafloxacin pharmacodynamics. (A and B) Concentration-response curves for extracellular bacteria in media at pH 7.4 or 5.5 or intracellularly exposed during 24 h to ciprofloxacin or finafloxacin at the indicated concentrations (expressed as multiples of the MIC at pH 7.4). (C) Evaluation of the number of bacteria over time of incubation under control conditions or with fluoroquinolones at the indicated concentrations in media at pH 7.4 or 5.5. Results on the graphs are mean values \pm SEM from at least three different experiments (each experiment performed in triplicate). CIP, ciprofloxacin; FIN, finafloxacin; Ctr, control condition without antibiotics.

Pharmacodynamic comparison between ciprofloxacin and finafloxacin. Differences in the pharmacodynamic profiles of two fluoroquinolones led us to study them in more detail. Based on the known contrasting pH on the activity of ciprofloxacin and finafloxacin, we compared their full concentration-response profiles against extracellular and intracellular bacteria (same as data presented in Fig. 3) with their effect on extracellular bacteria at pH 5.5. In this case, the variable slope was allowed for curve fitting to potentially better capture differences in concentration-effect relationships in these situations. Indeed, Fig. 4 shows marked differences between the two drugs depending on the extracellular pH. Ciprofloxacin displays a steep killing curve (Hill slope, -3.4) at pH 7.4, which becomes shallower at pH 5.5 (Hill slope, -1.3). The effect of pH was reversed for finafloxacin, with a steep curve at pH 5.5 (Hill slope, -3.9) and a shallower curve at pH 7.4 (Hill slope, -1.1). Interestingly, the Hill slope was even shallower intracellularly but similar between the two drugs (-0.3 for ciprofloxacin and -0.4 for finafloxacin, respectively), which indicates an impact of the intracellular environment independent of the local pH on their killing capacity.

We then examined the killing capacity of both fluoroquinolones over the first few hours of incubation in medium at pH 7.4 or 5.5, using concentrations causing a 0.5- to 1-log decrease in CFU numbers intracellularly based on concentration-response curves. As seen in Fig. 4C, ciprofloxacin killed bacterial cells faster at pH 7.4 than at pH 5.5, while the opposite was observed with finafloxacin.

Next, we monitored the kinetics of killing of intracellular bacteria using a very high but still clinically relevant concentration of 150 mg/liter ciprofloxacin and finafloxacin (Fig. 5A). The killing rate was higher in the first 3 h and slower at later time points for both antibiotics. Minimal duration of killing (MDK) was calculated from fitted curves for a reduction of 99% and 99.99% of the population (MDK_{99} and $\text{MDK}_{99.99}$). MDK_{99} were shorter for finafloxacin (4.6 h) than for ciprofloxacin (8.5 h) and markedly slowed down for both drugs when comparing the time needed to kill 99% of the entire population and then 99% of the survivors ($\text{MDK}_{99.99}$ of 23.5 h for finafloxacin and 27.2 h for ciprofloxacin). A biphasic killing curve is characteristic of heterogeneous bacterial populations containing persister cells, suggesting that metabolically more active cells are killed faster than dormant ones (32).

Analysis of the fluorescence of the reporter protein TIMERbac by flow cytometry was used to evaluate the metabolic status of intracellular bacteria (Fig. 5B to D) and allowed us to confirm its heterogeneity. Control samples of intracellular bacteria incubated in the presence of gentamicin at $3 \times \text{MIC}$, to avoid extracellular contamination,

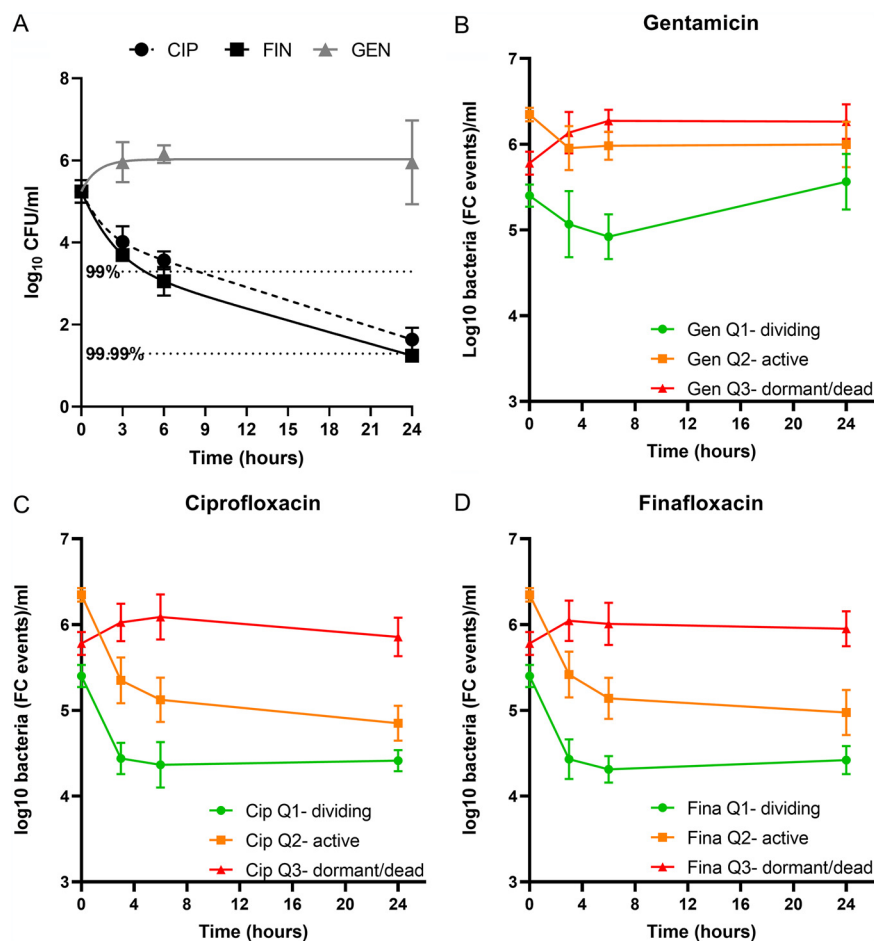


FIG 5 Intracellular time-kill curves comparing ciprofloxacin and finafloxacin. (A) Time-dependent killing of intracellular bacteria (presented as log₁₀ CFU per ml of J744 lysate from one well) by ciprofloxacin and finafloxacin at an extracellular concentration of 150 mg/liter or in the presence of gentamicin (at 3× MIC to avoid extracellular contamination). (B to D) In parallel with CFU determination, the same samples were analyzed by flow cytometry (FC) for TIMERbac fluorescence in the green and red channels as described in Fig. 2. Results on graphs are mean values ± standard deviations from at least three different experiments (each experiment performed in triplicate).

confirmed that their internalization results in an induction of dormancy, with the majority of bacteria being metabolically inactive even 6 h postinfection (Fig. 5B). However, at 24 h, the fraction of dividing cells started to increase ($P = 0.04$; unpaired t test between 6 and 24 h), suggesting that subpopulations of bacteria remain able to actively replicate within J744 macrophages after an adaptation period. Conversely, the numbers of dividing and/or metabolically active intracellular bacteria were significantly decreased within the first 3 h when the macrophages were exposed to high concentrations of ciprofloxacin or finafloxacin (Fig. 5C and D), and the number of metabolically active bacteria further decreased over time.

Notably, the number of bacteria detected by flow cytometry (FC events) decreases only three times when exposed to fluoroquinolones, while the CFU numbers decrease by several orders of magnitude (Fig. 5). This means that most of the bacteria detected by flow cytometry upon exposure to fluoroquinolones have lost their viability and/or culturability. However, changes in the fluorescence profile of bacterial cells still reveals which cells are more vulnerable to antibiotic action. The same biphasic profile was observed in comparisons of flow cytometry data with time-kill curves. Dividing bacteria were killed quickly during the first phase. Metabolically active but nondividing bacteria were killed mainly during the first hours but still at a slower pace during the second

phase. The number of dormant bacteria only marginally decreased after prolonged drug exposure.

DISCUSSION

In this study, we compared the activities of commonly used antibiotics for the treatment of UTIs, including a novel fluoroquinolone, finafloxacin, against extra- and intracellular infection by UPEC strain CFT073. We also determined the metabolic activity of intracellular bacteria and of the subpopulation that can escape antibiotic killing.

Using a J774 infection model, we found that intracellular UPEC is completely or partially protected from killing by several antibiotics, with nitrofurantoin and fluoroquinolones showing the best efficacy. Several reasons may lie behind the survival of intracellular bacteria during antibiotic treatment. They include inadequate pharmacokinetic properties (poor access to the infected subcellular compartment) or pharmacodynamic issues (lack of expression of activity intracellularly) (18), which may affect antibiotics from different classes in different ways.

When considering the activity of the different classes of antibiotics, our results are consistent with the study by Blango and Mulvey, who tested different antibiotics against another UPEC strain, UTI89, in a bladder cell culture-based assay and described nitrofurantoin and fluoroquinolones as the most effective drugs (24). However, the same study showed that in a mouse infection model, no drug was capable of eradicating the infection, whether it was highly (i.e., fluoroquinolones) or poorly (i.e., aminoglycosides) membrane permeable. Even disruption of infected mouse bladder tissue and a subsequent 4 h of incubation with ciprofloxacin did not eradicate all bacterial cells. These authors concluded that intracellular bacteria have become drug tolerant and are not efficiently killed even if the access of antibiotics to bacteria is not limiting. This is also what our data tend to suggest, pointing to the importance of examining the pharmacodynamic reasons for antibiotic failure in this context.

Among the factors that can affect the expression of antibiotic activity intracellularly, local pH and metabolic state of bacteria both can contribute to drug tolerance. It is well known that acidic pH, which is often present in the urinary tract as well as in the phagolysosomes containing intracellular bacteria, decreases the activity of most fluoroquinolones, such as ciprofloxacin, levofloxacin, and ofloxacin (33, 34). In contrast, the investigational fluoroquinolone finafloxacin shows improved activity at low pH, which makes it a good candidate for UTI treatment (35). The low pH in infected phagolysosomes that host bacteria might contribute to explaining why finafloxacin kills bacteria at lower multiples of MIC than ciprofloxacin and also with a faster initial killing rate. However, as with ciprofloxacin and other drugs, it remained much less efficient against intracellular than extracellular bacteria (either at pH 5.5 or pH 7.4). Therefore, we can conclude that the acidic pH that prevails in phagolysosomes is not sufficient to explain the major loss of efficacy observed against intracellular bacteria.

Our study of bacterial division and metabolic activity at the single bacterial cell level reveals the heterogeneity of the intracellular population, with the existence of a dormant pool of bacteria that do not respond to high concentrations of fluoroquinolones, in contrast to those that are actively multiplying and, to some extent, to those that do not multiply but remain metabolically active (Fig. 5B to D). This heterogeneity, also described for other intracellular pathogens, like *Salmonella* (36), would explain the biphasic shape of the time-kill curves (Fig. 5A) and the markedly reduced efficacy noticed in the concentration-kill curves (Fig. 4A and B), two hallmarks of persister subpopulations previously evidenced for intracellular *S. aureus* exposed to different classes of antibiotics in the same cellular model (12).

Our study suffers from some limitations. First, only one particular host cell line and pathogen strain were used. The J774 cell line certainly does not represent different host environments encountered by bacteria during UTI but is only a limited model of intracellular space. It is known that specific host-pathogen interactions have an impact on the outcome of the drug treatment (37, 38), but even with the same host-pathogen

pair, the outcome of drug treatment can be different depending on the time the drug treatment starts. In our study, the antibiotic treatment always starts after the end of phagocytosis, i.e., conditions where bacteria have stopped growing based on fluorescence dilution data. Thus, we cannot exclude that the outcome would be different if the antibiotic was added 24 h postinfection, when bacterial division seems to resume.

Second, there is an unavoidable flaw when the estimation of bacterial survival at a given time is done by plating and subsequent colony counting. This method does not allow one to distinguish between cells that do not give colonies because they died already during drug treatment or later on recovery plates (39). Some studies show that after treatment with DNA-damaging antibiotics, the postantibiotic environment of bacteria can largely influence whether they recover or die from the direct and/or secondary antibiotic-caused damage (40, 41). In the same line, we noticed a discrepancy between the number of CFU and the number of flow cytometry events recovered from antibiotic-treated infected cells, which indicates that part of the bacterial population reached a deeper level of dormancy that prevents or delays their regrowth on agar plates when removed from the stressful environment of the cells (42). This specific observation deserves additional experiments to explore the underlying mechanisms that are outside the scope of this work. Most likely, prolonged cell culture experiments, efficient drug removal methods, and time-lapse microscopy could, in the future, help to elucidate how well CFU plating estimates killing of UPEC by fluoroquinolones inside host cells.

Third, we exposed bacteria or infected cells to constant antibiotic concentrations, which do not mimic fluctuations in antibiotic concentrations over time observed in the serum of patients as well as in the urine, which may affect antibiotic efficacy as well as persister formation (43). This oversimplification is partially compensated by the concomitant examination of the effect of concentration or of time of exposure on antibiotic activity.

Despite these limitations, our study may contribute to the understanding of the reasons why antibiotics remain unable to eradicate UPEC in the context of UTIs. If we examine our data in a more clinically oriented perspective, we know that fluoroquinolones are concentration-dependent antibiotics and that C_{max} (maximal concentration) values in the serum of patients are at least 10 and even more than 100 times higher than MIC values of susceptible *E. coli* (44). Here, we show that extremely high antibiotic concentrations are needed to target intracellular bacteria, which can be achieved in the urine of patients if choosing the correct dosage regimen. The question remains whether we should consider serum or tissue concentrations for relapsing infection, in which case only fluoroquinolones will reach levels capable of killing 99% of the intracellular population among the drugs studied. Increasing treatment duration or increasing the dose has been suggested to reduce relapses in patients treated with fluoroquinolones (45–47), but a link with a possible effect on persistent intracellular subpopulations has not been established.

Our data suggest that fleroxacin is more effective than ciprofloxacin for eliminating intracellular slow-growing bacteria. Whether this translates to the results from *in vivo* studies should be investigated in clinical trials of UTI treatment with patient follow-up. This could confirm the potential of fleroxacin for eliminating intracellular UPEC and reducing the rate of infection relapse.

MATERIALS AND METHODS

Bacterial strain, growth conditions, and preparation of DMSO stocks. *E. coli* strain CFT073, which was originally isolated from the blood and urine of a woman with acute pyelonephritis (48), was transformed with pSC101 plasmid, carrying the TIMERbac (DsRed S197T variant) (31). For plasmid selection, kanamycin (25 mg/liter; Amresco) was added to the growth media. To prepare bacterial dimethyl sulfoxide (DMSO) stocks, overnight cultures were diluted 1:100 in fresh lysogeny broth (Lennox LB; Difco Laboratories) medium and grown aerobically to exponential phase. At an optical density at 600 nm (OD_{600}) of 0.8, DMSO was added to a final concentration of 8%, and the culture was immediately frozen in 120- μ l aliquots at -80°C . Stocks were stored up to 6 months.

Antibiotics susceptibility testing and 24-h concentration-response experiments. Bacteria, from DMSO stock, were diluted 1:100 in LB medium and grown aerobically for 24 h at 37°C with continuous shaking at 220 rpm. Susceptibility testing was done under neutral and acidic conditions in cation-adjusted Mueller-Hinton broth (CA-MHB; BD) and DMEM (ThermoFisher) supplemented with 10% fetal bovine serum (FBS; PAN Biotech), i.e., the medium used for experiments with infected cells. Acidic

condition (pH 5.5) was achieved by adding dropwise 1 M HCl. pH indicator strips were used for adjustment of the pH of media and its measurement after 18 h of incubation. MICs were determined by 2-fold serial microdilution in 96-well plates, according to Clinical and Laboratory Standards Institute (CLSI) guidelines (49), with readings performed after 18 h of incubation.

For antibiotic pharmacodynamic studies, bacteria from the overnight culture were inoculated into DMEM so that the initial inoculum was approximately 1×10^6 CFU/ml. DMEM was used for later comparison of results with intracellular pharmacodynamic studies. Afterwards, the antibiotic was added over a wide range of concentrations, corresponding to values from $0.003 \times$ MIC to $100 \times$ MIC. The incubation period was up to 24 h, at 37°C, in a 5% CO₂ atmosphere. At the end of the experiment, appropriate dilutions were made and 50 μ l plated on LB (lysogeny broth) agar plates. To prevent the carryover effect of tested antibiotics, 0.4% charcoal was added to the LB agar plates for antibiotic concentrations higher than MIC values. Results were expressed in change of CFU numbers per milliliter from the initial inoculum or absolute CFU numbers per volume unit.

Cell culture and viability. Experiments were performed with murine J774 macrophages (derived from reticulosarcoma [50]), obtained from Sandoz Forschung Laboratories, Vienna, Austria. Cells were cultured and maintained in RPMI 1640 (ThermoFisher) medium supplemented with 10% FBS at 37°C in a 5% CO₂ atmosphere. Macrophage viability was checked using trypan blue and lactate dehydrogenase (LDH) release tests.

Trypan blue test is based on the ability of trypan blue to penetrate and dye dead cells. J774 cells were first detached from the well bottom using 0.5% trypsin with EDTA (PAN Biotech) and resuspended in a total amount of 2 ml of DMEM. Next, 10 μ l of cell suspension was mixed with 10 μ l of trypan blue and incubated for 5 min. An automated cell counter (Invitrogen Countess) was used for assessing the percentage of cell viability.

LDH is a fairly stable cytosolic oxidoreductase enzyme that is released from damaged cells into the medium. Its activity was assayed using the LDH assay kit (Sigma-Aldrich), in which LDH reduces NAD to NADH, which is detected by colorimetric assay. After 24 h of incubation of infected cells in the presence of antibiotics, 20 μ l of culture medium was collected and placed immediately on ice. Medium from uninfected cells and cells exposed to 1% Triton for 1 h or 24 h were collected as well and used as positive controls. Samples were diluted $20 \times$ in a total volume of 100 μ l of buffer and master mix at a ratio of 1:1 (provided in the kit) in 96-well flat-bottom plates. Spectrophotometric readings were done at 450 nm, every 5 min, at 37°C, until the value of the most active sample is greater than the value of the highest standard (12.5 nmol/well), using a Synergy/Mx microplate reader (BioTek). LDH activity (milliunits/ml) was calculated according to the equation provided in the LDH kit, LDH activity = $B / (\text{reaction time} \times V) \times$ sample dilution factor, where B is the amount (nmol) of NADH generated between T_{initial} and T_{final} , reaction time is T_{final} minus T_{initial} (minutes), and V is sample volume (ml) added to the well.

Intracellular infection and assessment of antibiotic activity in cell culture. These experiments were performed using a protocol adapted from the one previously describing infection of J774 cells with *Staphylococcus aureus* (51). Bacteria, from DMSO stock, were diluted 1:100 in LB medium and grown for 48 h at 37°C under static conditions. The medium for intracellular experiments was DMEM with 10% FBS. Prior to the infection, bacteria were opsonized for half an hour in DMEM with 10% heat-inactivated human serum (obtained from healthy volunteers). This process was followed by phagocytosis, in which J774 cells were exposed to opsonized bacteria for 1 h at a bacterium/cell ratio of 50:1. Nonphagocytosed bacteria were eliminated by 1 h of incubation in the presence of 100 mg/liter gentamicin and $3 \times$ washing with phosphate-buffered saline (PBS) to eliminate gentamicin. The initial rate of infection was up to 10^6 CFU per milligram of cell protein. The activity of tested antibiotics against intracellular bacteria was analyzed by exposing infected J774 cells for 24 h to a wide range of antibiotic concentrations, corresponding to values from $0.003 \times$ to $100 \times$ MICs, which were predetermined in DMEM at neutral pH. After the incubation period with antibiotics, cells were washed $3 \times$ with PBS and then lysed in 1 ml distilled water. The cell lysate was further used for CFU counting by plating 50 μ l on LB agar plates without charcoal and for determination of total cell protein content by Lowry's assay (Bio-Rad DCTM protein assay). Antibiotic activity was expressed as the change of CFU number per milligram of cell protein from the initial postphagocytosis inoculum, in log₁₀ units.

Macrophage heterogeneity assessed with flow cytometry. Preparation of formaldehyde-fixed macrophages for flow cytometry analysis started with $3 \times$ washing of infected cells with PBS. The washing step was followed by cell detachment using 500 μ l of 0.5% trypsin with EDTA. A final volume of 1 ml was achieved by adding PBS to the cell suspension. After centrifugation at $300 \times g$ for 7 min to wash out the trypsin, the pellet was resuspended in 1 ml of 4% formaldehyde for 10 min. Fixative was further removed by one more centrifugation at $300 \times g$ for 7 min. Filtered PBS was used to resuspend the pellet in a final volume of 1 ml. Samples were kept on ice before analyzing them by flow cytometry (see the next paragraph).

Bacterial heterogeneity assessed with flow cytometry. Intracellular bacteria were obtained from infected macrophages at time zero and after 3, 6, and 24 h of incubation in the presence of tested antibiotics. Infected macrophages were first washed $3 \times$ with PBS and then lysed in 1 ml of filtered water. Samples were centrifuged at high speed ($900 \times g$, 7 min). The pellet was resuspended to the final volume of 1 ml PBS and kept on ice before analyzing. For growth resumption control, bacteria obtained from infected macrophages at time zero were inoculated into DMEM at a concentration of approximately 10^5 bacteria per ml. After 3, 6, and 24 h postinoculation, these extracellular growth resumption control bacteria were collected for fluorescence-activated cell sorting (FACS) analysis and used for defining their growth activity.

Both macrophage and bacterial samples were analyzed with an Attune NxT cytometer. TIMERbac fluorescence was recorded in two channels: green fluorescence excitation (Ex), 488 nm; emission (Em), 515 to 545 nm; red fluorescence Ex, 561 nm; Em, 577 to 593 nm.

Confocal microscopy. Intercellular heterogeneity also was assessed with the aid of confocal microscopy (LSM 710; Zeiss). For that purpose, J774 cells were grown in DMEM with 10% FBS in a 35-mm glass dish with a glass bottom, suitable for cell culture and fluorescence microscopy. Prior to live-cell imaging, Lyso Sensor green dye (DND-189; Invitrogen) was dissolved in cell culture medium (1 μ M), and cells were incubated at 37°C in a 5% CO₂ atmosphere. The dye helped in visualization of acidic cell compartments and determination of bacterial localization within macrophages. Lasers at 488 nm and 561 nm were used for excitation of TIMERbac protein, and a 458-nm laser was used for Lyso Sensor dye. Filters for collection of excited fluorescent light were 493 to 533 nm for green fluorescence, 566 to 616 nm for red fluorescence, and 474 to 552 nm for Lyso Sensor. The separated emissions of each fluorescence for TIMERbac protein and Lyso Sensor dye were acquired by multitrack scanning in which fluorophores were excited sequentially using one excitation wavelength at a time. Pictures were collected at 63 \times oil immersion magnification and then analyzed with Zen (2.3 SP1) software.

Antibiotics and main reagents. The following antibiotics were used as microbiological standards: fleroxacin (potency, 84.19%), provided by MerLion Pharmaceuticals GmbH (Berlin, Germany); gentamicin sulfate (potency, 60.79%), from AppliChem GmbH (Darmstadt, Germany); ampicillin sodium (potency, 97%), from Carl Roth GmbH (Karlsruhe, Germany); nitrofurantoin (potency, 98%), from Norwich Eaton Pharmaceuticals (Norwich, New York); and ciprofloxacin (potency, 98%), from Fluka, Sigma-Aldrich (St. Louis, Missouri). Trimethoprim (potency, 98%) and sulfamethoxazole (potency, 98%) were provided by Sigma-Aldrich (St. Louis, Missouri). For bacterial growth, LB (Difco Laboratories) medium was used, while for culturing of macrophage-like J774 cells, we used RPMI 1640 (R7388; Sigma) and DMEM (ref. 41966-052; ThermoFisher) supplemented with fetal bovine serum (Gibco, Life Technologies).

Statistical analysis. Statistical analyses were performed in GraphPad Prism version 8.4.3 (GraphPad Software). Pharmacodynamic parameters were calculated using Hill equations from concentration-response curves. *P* values lower than 0.05 were used to show significant statistical differences among results.

SUPPLEMENTAL MATERIAL

Supplemental material is available online only.

SUPPLEMENTAL FILE 1, PDF file, 0.8 MB.

ACKNOWLEDGMENTS

We thank Virginie Mohymont, Vasileios Yfantis, and Gang Wang for technical support or help in specific experiments and MerLion Pharmaceuticals GmbH (Berlin, Germany) for the kind gift of fleroxacin.

F.V.B. is Research Director of the Belgian Fonds de la Recherche Scientifique (FNRS-FRS). This work was supported by the Belgian Fonds de la Recherche Scientifique (FNRS-FRS), grant T.0189.16. Work of I.K. at Université Catholique De Louvain was supported by Dora Plus scholarship to I.K. from the Archimedes Foundation. The work at the University of Tartu was supported by the European Union from the European Regional Development Fund through the Centre of Excellence in Molecular Cell Engineering (2014-2020.4.01.15-0013) and by a grant from the Estonian Research Council (PRG335) to T.T.

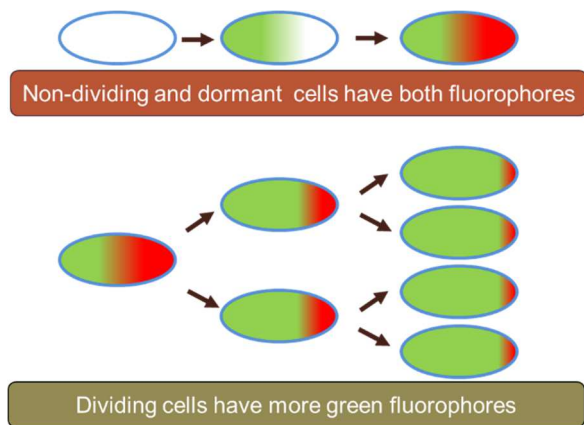
F.V.B. received a research grant from MerLion Pharmaceuticals unrelated to the work presented in this paper.

REFERENCES

- Schilling JD, Hultgren SJ. 2002. Recent advances into the pathogenesis of recurrent urinary tract infections: the bladder as a reservoir for uropathogenic *Escherichia coli*. *Int J Antimicrob Agents* 19:457–460. [https://doi.org/10.1016/S0924-8579\(02\)00098-5](https://doi.org/10.1016/S0924-8579(02)00098-5).
- Justice SS, Hung C, Theriot JA, Fletcher DA, Anderson GG, Footer MJ, Hultgren SJ. 2004. Differentiation and developmental pathways of uropathogenic *Escherichia coli* in urinary tract pathogenesis. *Proc Natl Acad Sci U S A* 101:1333–1338. <https://doi.org/10.1073/pnas.0308125100>.
- Palmer LM, Reilly TJ, Utsalo SJ, Donnenberg MS. 1997. Internalization of *Escherichia coli* by human renal epithelial cells is associated with tyrosine phosphorylation of specific host cell proteins. *Infect Immun* 65:2570–2575. <https://doi.org/10.1128/iai.65.7.2570-2575.1997>.
- Martinez JJ, Mulvey MA, Schilling JD, Pinkner JS, Hultgren SJ. 2000. Type 1 pilus-mediated bacterial invasion of bladder epithelial cells. *EMBO J* 19:2803–2812. <https://doi.org/10.1093/emboj/19.12.2803>.
- Bokil NJ, Totsika M, Carey AJ, Stacey KJ, Hancock V, Saunders BM, Ravasi T, Ulett GC, Schembri MA, Sweet MJ. 2011. Intramacrophage survival of uropathogenic *Escherichia coli*: differences between diverse clinical isolates and between mouse and human macrophages. *Immunobiology* 216:1164–1171. <https://doi.org/10.1016/j.imbio.2011.05.011>.
- Mysorekar IU, Hultgren SJ. 2006. Mechanisms of uropathogenic *Escherichia coli* persistence and eradication from the urinary tract. *Proc Natl Acad Sci U S A* 103:14170–14175. <https://doi.org/10.1073/pnas.0602136103>.
- Eto DS, Sundsbak JL, Mulvey MA. 2006. Actin-gated intracellular growth and resurgence of uropathogenic *Escherichia coli*. *Cell Microbiol* 8:704–717. <https://doi.org/10.1111/j.1462-5822.2006.00691.x>.
- Gilbert NM, O'Brien VP, Lewis AL. 2017. Transient microbiota exposures activate dormant *Escherichia coli* infection in the bladder and drive severe outcomes of recurrent disease. *PLoS Pathog* 13:e1006238. <https://doi.org/10.1371/journal.ppat.1006238>.
- Schreiber HL, Spaulding CN, Dodson KW, Livny J, Hultgren SJ, Hultgren SJ. 2017. One size doesn't fit all: unraveling the diversity of factors and interactions that drive *E. coli* urovirulence. *Ann Transl Med* 5:28. <https://doi.org/10.21037/atm.2016.12.73>.
- De Nisco NJ, Neugent M, Mull J, Chen L, Kuprasertkul A, de Souza Santos M, Palmer KL, Zimmern P, Orth K. 2019. Direct detection of tissue-resident

- bacteria and chronic inflammation in the bladder wall of postmenopausal women with recurrent urinary tract infection. *J Mol Biol* 431:4368–4379. <https://doi.org/10.1016/j.jmb.2019.04.008>.
11. Helaine S, Cheverton AM, Watson KG, Faure LM, Matthews SA, Holden DW. 2014. Internalization of Salmonella by macrophages induces formation of nonreplicating persisters. *Science* 343:204–208. <https://doi.org/10.1126/science.1244705>.
 12. Peyrusson F, Varet H, Nguyen TK, Legendre R, Sismeiro O, Coppée J-Y, Wolz C, Tenson T, Van Bambeke F. 2020. Intracellular Staphylococcus aureus persists upon antibiotic exposure. *Nat Commun* 11:2200. <https://doi.org/10.1038/s41467-020-15966-7>.
 13. Eisenreich W, Rudel T, Heesemann J, Goebel W. 2020. Persistence of intracellular bacterial pathogens—with a focus on the metabolic perspective. *Front Cell Infect Microbiol* 10:615450. <https://doi.org/10.3389/fcimb.2020.615450>.
 14. Balaban NQ, Helaine S, Lewis K, Ackermann M, Aldridge B, Andersson DI, Brynildsen MP, Bumann D, Camilli A, Collins JJ, Dehio C, Fortune S, Ghigo J-M, Hardt W-D, Harms A, Heinemann M, Hung DT, Jenal U, Levin BR, Michiels J, Storz G, Tan M-W, Tenson T, Van Melderen L, Zinkernagel A. 2019. Definitions and guidelines for research on antibiotic persistence. *Nat Rev Microbiol* 17:460. <https://doi.org/10.1038/s41579-019-0207-4>.
 15. Windels EM, Michiels JE, Fauvart M, Wenseleers T, Van den Bergh B, Michiels J. 2019. Bacterial persistence promotes the evolution of antibiotic resistance by increasing survival and mutation rates. *ISME J* 13: 1239–1251. <https://doi.org/10.1038/s41396-019-0344-9>.
 16. Levin-Reisman I, Ronin I, Gefen O, Braniss I, Shoshan N, Balaban NQ. 2017. Antibiotic tolerance facilitates the evolution of resistance. *Science* 355: 826–830. <https://doi.org/10.1126/science.aaj2191>.
 17. Kamaruzzaman NF, Kendall S, Good L. 2017. Targeting the hard to reach: challenges and novel strategies in the treatment of intracellular bacterial infections. *Br J Pharmacol* 174:2225–2236. <https://doi.org/10.1111/bph.13664>.
 18. Van Bambeke F, Barcia-Macay M, Lemaire S, Tulkens PM. 2006. Cellular pharmacodynamics and pharmacokinetics of antibiotics: current views and perspectives. *Curr Opin Drug Discov Dev* 9:218–230.
 19. Buyck JM, Luyckx C, Muccioli GG, Krause KM, Nichols WW, Tulkens PM, Van Bambeke F. 2017. Pharmacodynamics of ceftazidime/avibactam against extracellular and intracellular forms of *Pseudomonas aeruginosa*. *J Antimicrob Chemother* 72:1400–1409. <https://doi.org/10.1093/jac/dkw587>.
 20. Sandberg A, Jensen KS, Baudoux P, Van Bambeke F, Tulkens PM, Fridmott-Møller N. 2010. Intra- and extracellular activities of dioxacillin against *Staphylococcus aureus* in vivo and in vitro. *Antimicrob Agents Chemother* 54:2391–2400. <https://doi.org/10.1128/AAC.01400-09>.
 21. Lemaire S, Van Bambeke F, Tulkens PM. 2011. Activity of fluroxacin, a novel fluoroquinolone with increased activity at acid pH, towards extracellular and intracellular *Staphylococcus aureus*, *Listeria monocytogenes* and *Legionella pneumophila*. *Int J Antimicrob Agents* 38:52–59. <https://doi.org/10.1016/j.ijantimicag.2011.03.002>.
 22. Barcia-Macay M, Seral C, Mingeot-Leclercq M-P, Tulkens PM, Van Bambeke F. 2006. Pharmacodynamic evaluation of the intracellular activities of antibiotics against *Staphylococcus aureus* in a model of THP-1 macrophages. *Antimicrob Agents Chemother* 50:841–851. <https://doi.org/10.1128/AAC.50.3.841-851.2006>.
 23. Bongers S, Hellebrekers P, Leenen LPH, Koenderman L, Hietbrink F. 2019. Intracellular penetration and effects of antibiotics on *Staphylococcus aureus* inside human neutrophils: a comprehensive review. *Antibiotics* 8:54. <https://doi.org/10.3390/antibiotics8020054>.
 24. Blango MG, Mulvey MA. 2010. Persistence of uropathogenic *Escherichia coli* in the face of multiple antibiotics. *Antimicrob Agents Chemother* 54: 1855–1863. <https://doi.org/10.1128/AAC.00014-10>.
 25. González MJ, Zunino P, Scavone P, Robino L. 2020. Selection of effective antibiotics for uropathogenic *Escherichia coli* intracellular bacteria reduction. *Front Cell Infect Microbiol* 10:542755. <https://doi.org/10.3389/fcimb.2020.542755>.
 26. Bader MS, Loeb M, Leto D, Brooks AA. 2019. Treatment of urinary tract infections in the era of antimicrobial resistance and new antimicrobial agents. Taylor and Francis Inc, Abingdon, United Kingdom.
 27. Wagenlehner F, Nowicki M, Bentley C, Lückermann M, Wohlert S, Fischer C, Vente A, Naber K, Dalhoff A. 2018. Explorative randomized phase II clinical study of the efficacy and safety of fluroxacin versus ciprofloxacin for treatment of complicated urinary tract infections. *Antimicrob Agents Chemother* 62:e02317–17. <https://doi.org/10.1128/AAC.02317-17>.
 28. Chalhoub H, Harding SV, Tulkens PM, Van Bambeke F. 2020. Influence of pH on the activity of fluroxacin against extracellular and intracellular *Burkholderia thailandensis*, *Yersinia pseudotuberculosis* and *Francisella philomiragia* and on its cellular pharmacokinetics in THP-1 monocytes. *Clin Microbiol Infect* 26:1254.e1–1254.e8. <https://doi.org/10.1016/j.cmi.2019.07.028>.
 29. Mueller M, de la Peña A, Derendorf H. 2004. Issues in pharmacokinetics and pharmacodynamics of anti-infective agents: kill curves versus MIC. *Antimicrob Agents Chemother* 48:369–377. <https://doi.org/10.1128/AAC.48.2.369-377.2004>.
 30. Buyck JM, Lemaire S, Seral C, Anantharajah A, Peyrusson F, Tulkens PM, Van Bambeke F. 2016. In vitro models for the study of the intracellular activity of antibiotics. *Methods Mol Biol* 1333:147–157. https://doi.org/10.1007/978-1-4939-2854-5_13.
 31. Claudi B, Spröte P, Chirkova A, Personnic N, Zankl J, Schürmann N, Schmidt A, Bumann D. 2014. Phenotypic variation of *Salmonella* in host tissues delays eradication by antimicrobial chemotherapy. *Cell* 158:722–733. <https://doi.org/10.1016/j.cell.2014.06.045>.
 32. Brauner A, Fridman O, Gefen O, Balaban NQ. 2016. Distinguishing between resistance, tolerance and persistence to antibiotic treatment. *Nat Rev Microbiol* 14:320–330. <https://doi.org/10.1038/nrmicro.2016.34>.
 33. Schaeffer EM. 2015. Re: the influence of urinary pH on antibiotic efficacy against bacterial uropathogens. *J Urol* 193:151. <https://doi.org/10.1016/j.juro.2014.10.017>.
 34. Emrich NC, Heisig A, Stubbings W, Labischinski H, Heisig P. 2010. Antibacterial activity of fluroxacin under different pH conditions against isogenic strains of *Escherichia coli* expressing combinations of defined mechanisms of fluoroquinolone resistance. *J Antimicrob Chemother* 65: 2530–2533. <https://doi.org/10.1093/jac/dkq375>.
 35. McKeage K. 2015. Fluroxacin: first global approval. *Drugs* 75:687–693. <https://doi.org/10.1007/s40265-015-0384-z>.
 36. Helaine S, Thompson JA, Watson KG, Liu M, Boyle C, Holden DW. 2010. Dynamics of intracellular bacterial replication at the single cell level. *Proc Natl Acad Sci U S A* 107:3746–3751. <https://doi.org/10.1073/pnas.1000041107>.
 37. Helaine S, Holden DW. 2013. Heterogeneity of intracellular replication of bacterial pathogens. *Curr Opin Microbiol* 16:184–191. <https://doi.org/10.1016/j.mib.2012.12.004>.
 38. Bumann D. 2015. Heterogeneous host-pathogen encounters: act locally, think globally. *Cell Host Microbe* 17:13–19. <https://doi.org/10.1016/j.chom.2014.12.006>.
 39. Rasouly A, Nudler E. 2019. Reactive oxygen species as the long arm of bactericidal antibiotics. *Proc Natl Acad Sci U S A* 116:9696–9698. <https://doi.org/10.1073/pnas.1905291116>.
 40. Hong Y, Zeng J, Wang X, Drlica K, Zhao X. 2019. Post-stress bacterial cell death mediated by reactive oxygen species. *Proc Natl Acad Sci U S A* 116: 10064–10071. <https://doi.org/10.1073/pnas.1901730116>.
 41. Mok WWK, Brynildsen MP. 2018. Timing of DNA damage responses impacts persistence to fluoroquinolones. *Proc Natl Acad Sci U S A* 115: E6301–E6309. <https://doi.org/10.1073/pnas.1804218115>.
 42. Pu Y, Li Y, Jin X, Tian T, Ma Q, Zhao Z, Lin S, Chen Z, Li B, Yao G, Leake MC, Lo C-J, Bai F. 2018. ATP-dependent dynamic protein aggregation regulates bacterial dormancy depth critical for antibiotic tolerance. *Mol Cell* 73:143–156. <https://doi.org/10.1016/j.molcel.2018.10.022>.
 43. Seeger J, Michelet R, Kloft C. 2021. Quantification of persister formation of *Escherichia coli* leveraging electronic cell counting and semi-mechanistic pharmacokinetic/pharmacodynamic modelling. *J Antimicrob Chemother* 76:2088–2096. <https://doi.org/10.1093/jac/dkab146>.
 44. Pham TDM, Ziara ZM, Blaskovich MAT. 2019. Quinolone antibiotics. *Medchemcomm* 10:1719–1739. <https://doi.org/10.1039/c9md00120d>.
 45. Henry DC, Nenad RC, Iravani A, Tice AD, Mansfield DL, Magner DJ, Dorr MB, Talbot GH. 1999. Comparison of sparfloracin and ciprofloxacin in the treatment of community-acquired acute uncomplicated urinary tract infection in women. Sparfloracin Multicenter Uncomplicated Urinary Tract Infection Study Group. *Clin Ther* 21:966–981. [https://doi.org/10.1016/S0149-2918\(99\)80018-6](https://doi.org/10.1016/S0149-2918(99)80018-6).
 46. Hooton TM, Johnson C, Winter C, Kuwamura L, Rogers ME, Roberts PL, Stamm WE. 1991. Single-dose and three-day regimens of ofloxacin versus trimethoprim-sulfamethoxazole for acute cystitis in women. *Antimicrob Agents Chemother* 35:1479–1483. <https://doi.org/10.1128/AAC.35.7.1479>.
 47. González-Garay A, Velasco-Hidalgo L, Ochoa-Hein E, Rivera-Luna R. 2020. Efficacy and safety of quinolones for the treatment of uncomplicated urinary tract infections in women: a network meta-analysis. *Int Urogynecol J* 32:3–15. <https://doi.org/10.1007/s00192-020-04255-y>.

48. Mobley HL, Green DM, Trifillis AL, Johnson DE, Chippendale GR, Lockatell CV, Jones BD, Warren JW. 1990. Pyelonephritogenic *Escherichia coli* and killing of cultured human renal proximal tubular epithelial cells: role of hemolysin in some strains. *Infect Immun* 58:1281–1289. <https://doi.org/10.1128/iai.58.5.1281-1289.1990>.
49. CLSI. 2009. Methods for dilution antimicrobial susceptibility tests for bacteria that grow aerobically. Approved standard, 8th ed. Clinical and Laboratory Standards Institute, Wayne, PA.
50. Snyderman R, Pike MC, Fischer DG, Koren HS. 1977. Biologic and biochemical activities of continuous macrophage cell lines P388D1 and J774.1. *J Immunol* 119:2060–2066.
51. Seral C, Van Bambeke F, Tulkens PM. 2003. Quantitative analysis of gentamicin, azithromycin, telithromycin, ciprofloxacin, moxifloxacin, and oritavancin (LY333328) activities against intracellular *Staphylococcus aureus* in mouse J774 macrophages. *Antimicrob Agents Chemother* 47:2283–2292. <https://doi.org/10.1128/AAC.47.7.2283-2292.2003>.
52. Roholt K, Nielsen B, Kristensen E. 1974. Clinical pharmacology of pivampicillin. *Antimicrob Agents Chemother* 6:563–571. <https://doi.org/10.1128/AAC.6.5.563>.
53. Eshelman FN, Spyker DA. 1978. Pharmacokinetics of amoxicillin and ampicillin: crossover study of the effect of food. *Antimicrob Agents Chemother* 14:539–543. <https://doi.org/10.1128/AAC.14.4.539>.
54. Gilbert DN, Eubanks N, Jackson J. 1977. Comparison of amikacin and gentamicin in the treatment of urinary tract infections. *Am J Med* 62:924–929. [https://doi.org/10.1016/0002-9343\(77\)90662-3](https://doi.org/10.1016/0002-9343(77)90662-3).
55. Lindberg AA, Bucht H, Kallings LO. 1967. Treatment of chronic urinary tract infections with gentamicin. *J Clin Pathol* 20:760–766. <https://doi.org/10.1136/jcp.20.5.760>.
56. Odland B, Hartvig P, Fjellström KE, Lindström B, Bengtsson S. 1984. Steady state pharmacokinetics of trimethoprim 300 mg once daily in healthy volunteers assessed by two independent methods. *Eur J Clin Pharmacol* 26:393–397. <https://doi.org/10.1007/BF00548773>.
57. Wagenlehner FME, Münch F, Pilatz A, Bärman B, Weidner W, Wagenlehner CM, Straubinger M, Blenk H, Pfister W, Kresken M, Naber KG. 2014. Urinary concentrations and antibacterial activities of nitroxoline at 250 milligrams versus trimethoprim at 200 milligrams against uropathogens in healthy volunteers. *Antimicrob Agents Chemother* 58:713–721. <https://doi.org/10.1128/AAC.02147-13>.
58. Grose WE, Bodey GP, Loo TL. 1979. Clinical pharmacology of intravenously administered trimethoprim-sulfamethoxazole. *Antimicrob Agents Chemother* 15:447–451. <https://doi.org/10.1128/AAC.15.3.447>.
59. Schwartz DE, Rieder J. 1970. Pharmacokinetics of sulfamethoxazole plus trimethoprim in man and their distribution in the rat. *Chemotherapy* 15:337–355. <https://doi.org/10.1159/000220701>.
60. Carroll G, Brennan RV, Jacques R. 1955. Furadantin: human blood level and urinary concentration. *South Med J* 48:149–151. <https://doi.org/10.1097/00007611-195502000-00008>.
61. Wijma RA, Hüttner A, Koch BCP, Mouton JW, Muller AE. 2018. Review of the pharmacokinetic properties of nitrofurantoin and nitroxoline. *J Antimicrob Chemother* 73:2916–2926. <https://doi.org/10.1093/jac/dky255>.
62. Wagenlehner FME, Kinzig-Schippers M, Sörgel F, Weidner W, Naber KG. 2006. Concentrations in plasma, urinary excretion and bactericidal activity of levofloxacin (500 mg) versus ciprofloxacin (500 mg) in healthy volunteers receiving a single oral dose. *Int J Antimicrob Agents* 28:551–559. <https://doi.org/10.1016/j.ijantimicag.2006.07.026>.
63. Taubert M, Lückermann M, Vente A, Dalhoff A, Fuhr U. 2018. Population pharmacokinetics of finafloxacin in healthy volunteers and patients with complicated urinary tract infections. *Antimicrob Agents Chemother* 62:e02328-17. <https://doi.org/10.1128/AAC.02328-17>.
64. Dalhoff A, Schubert S, Vente A. 2017. Pharmacodynamics of finafloxacin, ciprofloxacin, and levofloxacin in serum and urine against TEM- and SHV-type extended-spectrum- β -lactamase-producing *Enterobacteriaceae* isolates from patients with urinary tract infections. *Antimicrob Agents Chemother* 61:e02446-16. <https://doi.org/10.1128/AAC.02446-16>.



Supplementary Figure 1. Schematic principle of TIMERbac reporter. Constitutively expressed protein has branched maturation pathway with rapid emergence of green fluorophores and delayed formation of red fluorophores.



Supplementary Figure 2. Presence of small colony variants of CFT073, detected when extracellular concentration of gentamicin was 1 mg/L (equal to 1 x MIC).